

Detection of N¹⁵NH⁺ in L1544

L. Bizzocchi¹, P. Caselli², and L. Dore¹

¹ Dipartimento di Chimica “G. Ciamician”, Università di Bologna, via F. Selmi 2, I-40126 Bologna (Italy) e-mail: [luca.bizzocchi, luca.dore]@unibo.it

² School of Physics and Astronomy, University of Leeds, Leeds LS2 9JT (UK) e-mail: P.Caselli@leeds.ac.uk

Preprint online version: August 22, 2021

ABSTRACT

Context. Excess levels of ¹⁵N isotopes which have been detected in primitive solar system materials are explained as a remnant of interstellar chemistry which took place in regions of the protosolar nebula.

Aims. Chemical models of nitrogen fractionation in cold clouds predict an enhancement in the gas-phase abundance of ¹⁵N-bearing molecules, thus we have searched for ¹⁵N variants of the N₂H⁺ ion in L1544, which is one of the best candidate sources for detection owing to its low central core temperature and high CO depletion.

Methods. With the IRAM 30 m telescope we have obtained deep integrations of the N¹⁵NH⁺ (1 – 0) line at 91.2 GHz.

Results. The N¹⁵NH⁺ (1 – 0) line has been detected toward the dust emission peak of L1544. The ¹⁴N/¹⁵N abundance ratio in N¹⁵NH⁺ resulted 446 ± 71, very close to the protosolar value of ~ 450, higher than the terrestrial ratio of ~ 270, and significantly lower than the lower limit in L1544 found by Gerin et al. (2009, ApJ, 570, L101) in the same object using ammonia isotopologues.

Key words. ISM: clouds – molecules – individual object (L1544) – radio lines: ISM

1. Introduction

The isotopic ¹⁴N/¹⁵N ratio has been measured in a variety of solar system bodies, including giant and rocky planets, comets, and meteorites. Its value exhibits large variations, depending on the selected object and the source for the measurement (Owen et al. 2001; Meibom et al. 2007), with the global Jovian value of 450 ± 100 representing probably the best approximation of the protosolar value (Fouchet et al. 2004). This value differs significantly from the terrestrial one of ~ 272, and even larger ¹⁵N excess was found in primitive solar system materials like meteorites, interplanetary dust particles (IDPs), and cometary dust particles returned by the *Stardust* mission (Alexander et al. 1998; Messenger 2000; Messenger et al. 2003; Aléon & Robert 2004; Clayton & Nittler 2004; McKeegan et al. 2006); to date, the largest ¹⁵N enhancement detected is a ¹⁴N/¹⁵N ratio of 65 ± 11 (corresponding to about four times the terrestrial abundance of ¹⁵N) in the hotspots of the meteorite Bells (Busemann et al. 2006). The lack of any significant ¹³C enhancement in the material with the largest ¹⁵N content (Floss et al. 2004) rules out a nucleosynthetic origin for the nitrogen fractionation and suggests that, as with deuterium, the ¹⁵N-rich material results from low-temperature gas-phase ion-molecule reactions and catalysis on cold interstellar dust grains (e.g. Charnley & Rodgers 2002).

The early model of ¹⁵N fractionation in the interstellar medium (ISM) developed by Terzieva & Herbst (2000) predicted only a modest enrichment and was thus unable to account for such large enhancements. Subsequently, Charnley & Rodgers (2002) showed that much higher ¹⁵N/¹⁴N ratios can be generated in high-density cores, where CO is depleted onto dust grains, but N₂ remains in the gas phase, as appears to be the case in many pre-stellar cores (Caselli et al. 1999; Bergin et al. 2002; Tafalla et al. 2002; Bergin & Tafalla 2007). The key fractionation processes are the exothermic reactions (Terzieva & Herbst 2000)



which, at low temperatures, drive ¹⁵N into molecular nitrogen through the dissociative recombination of dyazenilium ions (Molek et al. 2007). Under normal interstellar conditions, ¹⁴N and ¹⁵N atoms are continuously exchanged into molecular nitrogen through the sequence



but in heavily depleted regions, there is insufficient OH to drive the above sequence. In these conditions, ¹⁵N is preferentially incorporated into gas-phase N₂ through the dissociative recombination of ¹⁵NNH⁺ and N¹⁵NH⁺, and into solid NH₃ through the production of ¹⁵N⁺ via ¹⁵NN + He⁺, successive hydrogenation of ¹⁵N⁺, production of ¹⁵NH₃ and freeze-out onto dust grain surfaces (Charnley & Rodgers 2002; Rodgers & Charnley 2008b). Assuming selective depletion, this chemistry leads to accretion of ammonia ice with high ¹⁵N enrichment, up to one order of magnitude with respect to the elemental ¹⁵N/¹⁴N ratio, more than sufficient to explain the largest measured enhancements. However, this theoretical model is still to some extent speculative, due to the paucity of observational data on key ¹⁵N-bearing molecules in dense prestellar cores. In this context, the observation of ¹⁵N-containing

diazanylium ion in selectively depleted dark clouds is an efficient probe to assess if the nitrogen fractionation process is at work in the way described, as the model predicts an enhancement in the abundance of both $^{15}NNH^+$ and $N^{15}NH^+$.

Previous searches of isotopic variants of N_2H^+ have been carried out a long time ago (Womack et al. 1992; Linke et al. 1983) and the detection was successful only toward massive star forming regions, owing to the low sensitivity achieved and also because of the selection of sources, which did not concentrate on heavily CO-depleted, centrally concentrated cores (not known at that time). To date, no observational data on $^{15}NNH^+$ and $N^{15}NH^+$ in the ISM are available, thus we initiated a survey of ^{15}N -diazanylium in cold quiescent clouds, starting from L1544, which we expected to be a very good candidate source for the detection because (i) the deuterium enhancement in this source is very large ($N_2D^+/N_2H^+ \sim 0.25$, Crapsi et al. 2007); (ii) deuterated species are excellent tracers of the high density gas in the center of the core (Caselli et al. 2002a), where CO is more heavily depleted and thus where the highest ^{15}N enhancement is expected from the above reasoning; and (iii) recent observations revealed that its central region has a temperature of only 5.5 K (Crapsi et al. 2007), thus, due to the small zero-point energy changes associated with ^{15}N -fractionation, these low temperatures are expected to yield higher $^{15}N/^{14}N$ ratios. We report here the positive detection of the $N^{15}NH^+$ ($1-0$) emission at 91.2 GHz in this cold dense molecular core.

2. Observations

The millimetre and submillimetre spectra of $N^{15}NH^+$ and $^{15}NNH^+$ were recently investigated in the laboratory by Dore et al. (2009), and the data were used by the authors to produce accurate hyperfine line lists adopting the quadrupole coupling and spin-rotation constant of the parent species (Caselli et al. 1995). The same data have also been included in the Cologne Database for Molecular Spectroscopy (CDMS, Müller et al. 2001, 2005), where lists of hyperfine-free rotational transitions of ^{15}N -containing isotopologues of the diazenylium ion are also presented.

The observations toward the quiescent Taurus starless core L1544 were performed with the IRAM 30 m antenna, located at Pico Veleta (Spain) during one observing session in June 2009. Since the ($1-0$) transitions of $N^{15}NH^+$ and $^{15}NNH^+$ have rest frequencies of 91205.6952 MHz and 90263.8360 MHz, respectively, it was not possible to observe both lines simultaneously with the same detector settings due to the current limitations in the telescope hardware. In the initial observing strategy, a splitting of the telescope time into two separate runs was planned; but owing to the unstable weather conditions, we decided to employ the whole allocated time integrating the $N^{15}NH^+$ ($1-0$) transition in order to obtain a spectrum with sufficient signal-to-noise ratio. We used the EMIR receivers in the E090 configuration, observing the $N^{15}NH^+$ ($1-0$) line in the lower-inner sideband. The observations were performed in frequency switching mode, with a throw of ± 7 MHz; the backend used was the VESPA correlator set to a spectral resolution of 20 kHz (corresponding to 0.065 km s^{-1}) and spectral bandpass of 20 MHz. Telescope pointing was checked every two hours on nearby planets and bright radio quasars and was found accurate to $\sim 4''$; the half power beam width (HPBW) was $27''$. Scans were taken toward the peak of the 1.3 mm continuum dust emission of L1544 (Caselli et al. 2002a), the adopted coordinates were $RA(2000) = 05^h04^m17.21^s$, $Dec(2000) = 25^\circ10'42.8''$. We integrated for a total of 27.25 hours, with two orthogonal polarizations simultaneously observed and averaged together to produce the final spectrum. The rms noise level achieved was about 2.5 mK, allowing for a clear detection of $N^{15}NH^+$ ($1-0$) emission line toward L1544, as illustrated by Fig. 1. The spectrum is presented in units of T_{mb} and was corrected assuming a source filling factor of unity and using the forward and main beam efficiencies appropriate for 91 GHz, $F_{eff} = 0.95$ and $B_{eff} = 0.75$, respectively.

3. Results

The data processing was done with the GILDAS¹ software (e.g. Pety 2005); due to the wavy background produced by the frequency switching observing method, extensive polynomial baseline subtraction had to be applied to obtain reasonable flat spectra. Since the nuclear spin of ^{15}N is $\frac{1}{2}$, $N^{15}NH^+$ has only one quadrupolar nucleus, ^{14}N with $I = 1$, thus its ($1-0$) rotational lines are split into a triplet, making its detection easier than of the parent species whose hyperfine structure is spread over seven components (Caselli et al. 1995).

Figure 1 displays the averaged spectrum taken toward L1544. The two stronger $F = 2-1$ and $F = 1-1$ transitions are clearly seen, while the weak $F = 0-1$ component is detected at 2σ level. Average line parameters can be estimated by fitting Gaussian profiles to the detected lines with the HFS routine implemented in CLASS, which allows to take into account the hyperfine components self-consistently. Adopting the hyperfine splittings and intensities of the $J = 1-0$ transition calculated by Dore et al. (2009), the HFS fit gives a systemic velocity $V_{LSR} = 7.299 \pm 0.017 \text{ km s}^{-1}$ and an intrinsic line width $\Delta v = 0.533 \pm 0.054 \text{ km s}^{-1}$; it also indicates, as expected, a low optical depth ($\tau < 0.1$) for the line, thus no information on the excitation temperature T_{ex} can be derived from the observational data. The results of the HFS fit are summarised in Table 1, and the resulting spectral profile is superimposed in Fig. 1 as a dotted trace.

The column density of $N^{15}NH^+$ has been calculated from the integrated $N^{15}NH^+$ line intensity of the strongest $F = 2-1$ component, which exhibits the best spectral profile. The Gaussian fit gives $\int T_{mb} dv = 14.2 \pm 1.1 \text{ mK km s}^{-1}$ and $\Delta v = 0.575 \pm 0.055 \text{ km s}^{-1}$. We adopted the constant excitation temperature approximation (Caselli et al. 2002b), assuming a T_{ex} value of 5.0 K as derived from observations of the N_2H^+ ($1-0$) hyperfine structure toward the same object and the same offset position (Caselli et al. 2002a). From the solution of the radiative transfer equation with the assumption of optically thin emission, one has the following expression for the total column density (Caselli et al. 2002b)

$$N_{tot} = \frac{8\pi\nu^3}{c^3 A} \frac{Q_{sr}(T_{ex})}{2F_u + 1} \left[\exp\left(\frac{h\nu}{kT_{ex}}\right) - 1 \right]^{-1} \exp\left(\frac{E_u}{kT_{ex}}\right) \frac{\int T_{mb} dv}{J_\nu(T_{ex}) - J_\nu(T_{bg})}, \quad (4)$$

¹ See GILDAS home page at the URL: <http://www.iram.fr/IRAMFR/GILDAS>.

where A is the emission Einstein's coefficient for the hyperfine transition, $J_\nu(T)$ is the radiation temperature of a black body at temperature T , E_u is the upper state energy, and $Q_{sr}(T_{ex})$ is the spin-rotational partition function for the excitation temperature obtained by summing over all energy levels of importance.

The A coefficient for the $F = 2 - 1$ hyperfine line was calculated from the formula given by Dore et al. (2009) and with the weighted average of the literature values of the N¹⁵NH⁺ dipole moments, $\mu = 3.31 \pm 0.20$ D (Havenith et al. 1990, Table II), resulting $A = 3.23 \pm 0.40 \cdot 10^{-5} \text{ s}^{-1}$. Substitution of all terms of Eq. (4) gives a total column density of N¹⁵NH⁺ toward L1544 of $(4.1 \pm 0.5) \cdot 10^{10} \text{ cm}^{-2}$, where the estimated uncertainty is obtained by propagating the errors on A , T_{ex} , and the integrated intensity derived from the present observations.

4. Discussion

The column density of the main dyazenium ion derived toward the “dust peak” of L1544 by Crapsi et al. (2005) is $(18.3 \pm 1.9) \cdot 10^{12} \text{ cm}^{-2}$ and thus the resulting $[\text{N}_2\text{H}^+/\text{N}^{15}\text{NH}^+]$ abundance ratio is 446 ± 71 , which is well comparable with the recognised protosolar value of the ¹⁴N/¹⁵N ratio, as measured in the Jupiter atmosphere (~ 450 , Fouchet et al. 2004), or in osbornite-bearing inclusions from meteorites (~ 420 , Meibom et al. 2007).

Very recently Gerin et al. (2009) reported on a search for ¹⁵NH₂D in dense cores, with the aim of measuring the nitrogen isotopic ratio in the ISM. They observed several sources, including L1544, obtaining ¹⁴N/¹⁵N ratios ranging from 350 and 850. In L1544 the detection of ¹⁵NH₂D was not achieved, leading to an estimation of a lower limit of 700 for this ratio. The value we obtained for N₂H⁺ is nearly two times smaller than this estimate, indicating that the mechanism of nitrogen fractionation at work in these cold dense cores produces marked differences of ¹⁵N enhancement among different chemical species.

The time dependent coupled gas/solid chemical model of Charnley & Rodgers (2002) (see also Rodgers & Charnley 2008b) predicts that at the end of evolution significant amounts of ¹⁵N-rich ammonia are frozen onto ice mantles, while the gas phase becomes enriched at early times, before the complete depletion of molecules. Improved models (Rodgers & Charnley 2008a; Gerin et al. 2009) which include additional ion/neutral and neutral/neutral reaction channels predict that assuming typical dense-core parameters, ¹⁵N enrichment of ammonia is only moderate in the gas phase, while much stronger enrichment is expected for N₂H⁺ (Gerin et al. 2009, figure 2). Thus, it appears that our finding is not compatible with the above picture, given that the $[\text{N}_2\text{H}^+]/[\text{N}^{15}\text{NH}^+]$ ratio in L1544 is consistent with the ¹⁴N/¹⁵N abundance ratio in the local ISM (Wilson & Rood 1994). In any case, further observations are needed to effectively test these chemical models. In particular, the detection of the other isotopologue ¹⁵NNH⁺ will be very interesting, since due to the different exothermicities of the reactions (1) and (2), the two ions should be fractionated to a different degree. Rodgers & Charnley (2004) predicted a gas-phase ratio $[\text{N}^{15}\text{NH}^+]/[\text{N}^{15}\text{NNH}^+]$ of about 2, which differs significantly from the equal abundances that would exist without the fractionation mechanism. A tentative determination of this ratio is found in Linke et al. (1983) who obtained 1.25 in DR 21 (OH), but it is likely that new determinations in centrally CO-depleted cores might yield higher values.

Acknowledgements. The authors thank the anonymous referee and the editor for their helpful observations. We are grateful to the IRAM 30m staff for their support during the observations. LB acknowledges travel support to Pico Veleta from TNA Radio Net project funded by the European Commission within the FP7 Programme. LD acknowledges support from the University of Bologna (RFO funds).

References

- Aléon, J. & Robert, F. 2004, *Icarus*, 167, 424
 Alexander, C. M. O., Russell, S. S., Arden, J. W., et al. 1998, *Meteor. Planet. Sci.*, 33, 603
 Bergin, E. A., Alves, J., Huard, T., & Lada, C. J. 2002, *ApJ*, 570, L101
 Bergin, E. A. & Tafalla, M. 2007, *ARA&A*, 45, 339
 Busemann, H., Young, A. F., Alexander, C. M. O., et al. 2006, *Science*, 312, 727
 Caselli, P., Myers, P. C., & Thaddeus, P. 1995, *ApJ*, 455, L77
 Caselli, P., Walmsley, C. M., Tafalla, M., Dore, L., & Myers, P. C. 1999, *ApJ*, 523, L165
 Caselli, P., Walmsley, C. M., Zucconi, A., et al. 2002a, *ApJ*, 565, 331
 Caselli, P., Walmsley, C. M., Zucconi, A., et al. 2002b, *ApJ*, 565, 344
 Charnley, S. B. & Rodgers, S. D. 2002, *ApJ*, 569, L133
 Clayton, D. D. & Nittler, L. R. 2004, *ARA&A*, 42, 39
 Crapsi, A., Caselli, P., Walmsley, C. M., et al. 2005, *ApJ*, 619, 379
 Crapsi, A., Caselli, P., Walmsley, M. C., & Tafalla, M. 2007, *A&A*, 470, 221
 Dore, L., Bizzocchi, L., Degli Esposti, C., & Tinti, F. 2009, *A&A*, 496, 275
 Floss, C., Stadermann, F. J., Bradley, J., et al. 2004, *Science*, 303, 1355
 Fouchet, T., Irwin, P. G. J., Parrish, P., et al. 2004, *Icarus*, 172, 50
 Gerin, M., Marcelino, N., Biver, N., et al. 2009, *A&A*, 498, L9
 Havenith, M., Zwart, E., Meerts, W. L., & ter Meulen, J. J. 1990, *J. Chem. Phys.*, 93, 8446
 Linke, R. A., Guélin, M., & Langer, W. D. 1983, *ApJ*, 271, L85
 McKeegan, K. D., Aléon, J., Bradley, J., et al. 2006, *Science*, 314, 1724
 Meibom, A., Krot, A. N., Robert, F., et al. 2007, *ApJ*, 656, L33
 Messenger, S. 2000, *Nature*, 404, 968
 Messenger, S., Stadermann, F. J., Floss, C., Nittler, L. R., & Mukhopadhyay, S. 2003, *Space Sci. Rev.*, 106, 155
 Molek, C. D., McLain, J. L., Poterya, V., & Adams, N. G. 2007, *J. Phys. Chem. A*, 111, 6760
 Müller, H. S. P., Schlöder, F., Stutzki, J., & Winnewisser, G. 2005, *J. Mol. Spectrosc.*, 742, 215
 Müller, H. S. P., Thorwirth, S., Roth, D. A., & Winnewisser, G. 2001, *A&A*, 370, L49
 Owen, T., Mahaffy, P. R., Niemann, H. B., Atreya, S., & Wong, M. 2001, *ApJ*, 553, L77
 Pety, J. 2005, in *EdP-Sciences Conference Series*, ed. F. Casoli, T. Contini, J. Hameury, & L. Pagani, Vol. SF2A-2005, 721
 Rodgers, S. D. & Charnley, S. B. 2004, *MNRAS*, 352, 600

Rodgers, S. D. & Charnley, S. B. 2008a, ApJ, 689, 1448
 Rodgers, S. D. & Charnley, S. B. 2008b, MNRAS, 385, L48
 Tafalla, M., Myers, P. C., Caselli, P., Walmsley, C. M., & Comito, C. 2002, ApJ, 569, 815
 Terzieva, R. & Herbst, E. 2000, MNRAS, 317, 563
 Wilson, T. L. & Rood, R. T. 1994, ARA&A, 32, 191
 Womack, M., Ziurys, L. M., & Wyckoff, S. 1992, ApJ, 387, 417

Table 1. Results of the hyperfine fit on the observed spectral profile of the $N^{15}NH^+$ ($1-0$) transition toward L1544. Numbers in parentheses refer to 1σ uncertainties in units of the last quoted digit.

Line $F' - F$	Rest frequency ^a (MHz)	A coefficient $10^5 s^{-1}$	V_{LSR} ($km s^{-1}$)	$\int T_{mb} dv$ ($mK km s^{-1}$)	Δv ($km s^{-1}$)	$10^3 \tau^b$
0 - 1	91 208.5162	3.23(40)	-1.971 ^c	2.68(34)	...	2.31(20)
2 - 1	91 205.9908	3.23(40)	6.329(17)	13.4(17)	0.533(54) ^d	11.6(11)
1 - 1	91 204.2602	3.23(40)	12.018 ^c	8.1(10)	...	6.95(63)

^a From Dore et al. (2009).

^b Optical depth derived assuming $T_{ex} = 5.0 \pm 0.1$ K from Caselli et al. (2002a).

^c The hyperfine splitting with respect to $F = 2 - 1$ component was kept fixed in the HFS analysis.

^d Gaussian FWHM. Assumed equal for all the components.

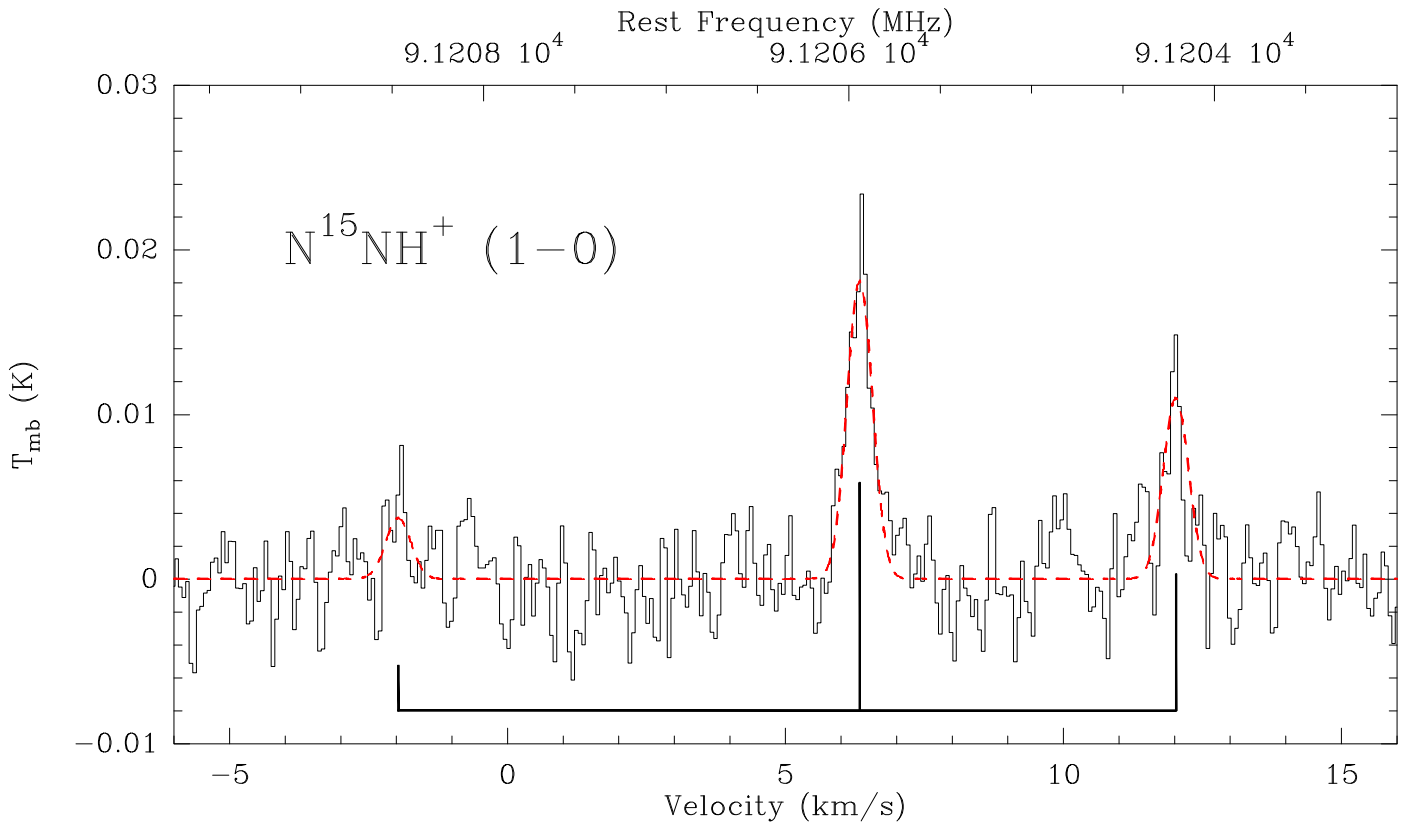


Fig. 1. Spectrum of the $N^{15}NH^+$ ($1-0$) transition observed toward L1544 (grey trace), and computed spectral profile resulting from the HFS fits (red dashed trace). The superimposed histogram (black trace) indicates the position and relative intensity of the hyperfine components.